

The use of smart material of nanofluid for heat transfer enhancement in microtube with helically spiral rib and groove

Open

Thillai Mugilan^{1,*}, Nor Azwadi Che Sidik^{1,2}, Wan Mohd Arif Aziz Japar²

¹ Faculty of Mechanical Engineering, Universiti Teknologi Malaysia, 81310 UTM Skudai, Johor, Malaysia

² Malaysia-Japan International Institute of Technology (MJIIT), Universiti Teknologi Malaysia Kuala Lumpur, Malaysia

ARTICLE INFO

ABSTRACT

Article history:

Received 27 February 2017

Received in revised form 26 May 2017

Accepted 27 May 2017

Available online 25 June 2017

Keywords:

Volume Fraction, Al₂O₃/water Nanofluid,

Helical Rib, Nusselt number,

Microchannel

This paper presents a numerical work on forced convection heat transfer of Al₂O₃/water nanofluid in a helically ribbed and grooved horizontal microtube using ANSYS FLUENT. The Reynolds numbers were selected from 100 to 1000. Two different geometries of spiraled and grooved tube with diameter 0.02m and length 10mm length and constant heat flux 5000 W/m² applied on surrounding wall have been considered. The volume fraction of nanoparticle considered were set at 0%, 1%, 2%, and 3%. The computational results showed that the heat transfer coefficient and Nusselt number were enhanced with the value of volume fraction.

Copyright © 2017 PENERBIT AKADEMIA BARU - All rights reserved

1. Introduction

Heat transfer is a kind of energy observation that is continuously researched around the world. Convective heat transfer is the transfer of heat from one place to another by the movement of fluids. Many researches have focused their attention on heat transfer enhancement in especially in heat exchanger devices with aims to reduce operational cost and size, or to increase the heat efficiency. One way to enhance the heat transfer in heat exchanger ducts is by increasing the heat transfer area, flow turbulization or enhancement of thermophysical properties of the fluid[1].

Many studies have documented that the application of ribs or groove in a tube could enhance the heat transfer, however at the same time increase the pressure drop [2-6]. For the case of laminar flow, several researchers concluded that the heat transfer and pressure drop were not greatly affected by the enhanced tubes. Ravigururajan and Bergles [7] tested the effect of pitch, ribs height and helical angle parameters on heat transfer enhancement and pressure drop for helical geometries. They found that, for micro-ribs with various angles and pitches, the analogy method did not give accurate correlations. Siddique and Alhazmy [8] tested a tube with several of angles and

* Corresponding author.

E-mail address: mugilan@gmail.com (Thillai Mugilan)

groove numbers. They observed a variation in the friction factor at an increasing of Re number and non-uniform trend of heat transfer characteristics was found. Four micro-fin tubes with various Re were investigated by Han and Lee [9]. They observed that, as far as the efficiency index is concerned, the tube with smaller helical angle and higher relative roughness appeared to have better heat transfer performance than the tubes with smaller relative roughness and larger helical angle.

The mechanism of heat transfer was explained in a report by Li *et al.* [10] by visualization of the flow in helically finned tubes. They found that laminar flow with bubbles in a parabolic pattern and due to random separation of vortices in the turbulent regime, this pattern broke down. In another study, Fahed *et al.* [11] showed that the heat transfer and pressure drop in micro fin tubes were just slightly higher than in plain tubes. They recommended that the micro fin tubes shall not be used for laminar flow conditions. Generally, most of the papers available in literature describe the results obtained from experimental study.

In recent years, several researchers have focused on heat transfer enhancement by modifying the thermo-physical properties of the working fluid. Nanofluid is an engineered colloidal suspension of nanoparticles in a base fluid, have been applied in many real engineering applications such as the photonics, transportation, electronics, and energy supply industries [12-16] due to its enhanced thermal conductivity and the convective heat transfer coefficient compared to the base fluid[17-20]. Yang *et al.* [21] investigated the convective heat transfer coefficient of nanoparticle dispersion in a fluid for laminar flow in a horizontal tube heat exchanger. The results indicated that the heat transfer coefficient increased at higher Reynold numbers and particle volume concentrations.

Wen and Ding [22] studied the convective heat transfer in the entrance region under laminar regime using aluminium oxide nanofluid in a circular tube with constant heat flux. Migration of nanoparticles and the subsequent disturbance of the boundary layer were attributed to the enhancement in heat transfer rate. Zeinali Heris *et al.* [23] compared the heat transfer enhancement by copper and aluminium oxide nanofluids in laminar pipe flow under constant wall temperature conditions and found the aluminium oxide nanofluid better than the copper oxide nanofluid.

In the present study, the main concern is to investigate the effects of different concentration on heat transfer performance of Al_2O_3 -water based nanofluid flow in horizontal helically ribbed or grooved microtube subject to constant wall heat flux. The heat transfer coefficient and pressure drop is tabulated and discussed.

2. Methodology

2.1 CAD model

The fluid geometry inside a helically ribbed and grooved cylindrical microtube in a horizontal position is considered in the current study.

Table 1
Dimensions of the Geometry

Item	Ribbed Pipe	Grooved Pipe
Inner Diameter	200 μ m	200 μ m
Length	10mm	10mm
Rib/Groove diameter	40 μ m	40 μ m
Pitch Length	5mm	5mm
Revolution	2	2
Number of Starts	4	4

The design parameters for both helically ribbed and grooved geometry is maintained constant due to comparison reason. The dimension used is given in Table 1. The 3-dimensional geometry is modeled using Solidworks 2010 as shown in Fig. 1. A constant heat flux is applied to the tube wall which is assumed to be applied directly to the fluid surface due to negligible thickness of the pipe wall.

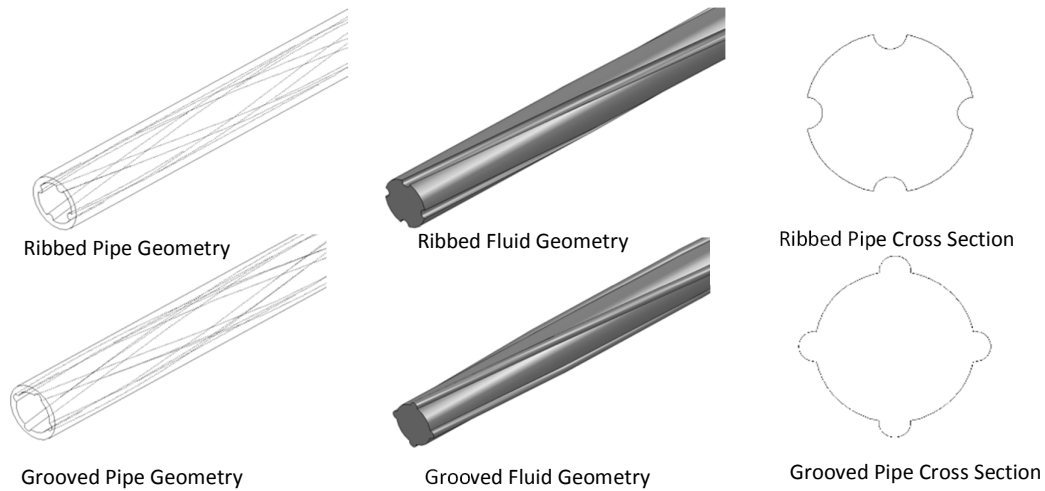


Fig. 1. Characteristic geometry, dimensions and boundary of the heat pipe

2.2 Meshing

Both 3-dimensional geometries were meshed using the same parameters. Proximity and curvature settings were chosen in the sizing function. The relevance center and the smoothing of the mesh is chosen to be medium where else all the other settings remains default. The proximity size function is also remained at default values. The mesh was manually created using edge sizing for all separate edges as shown in Fig. 2.

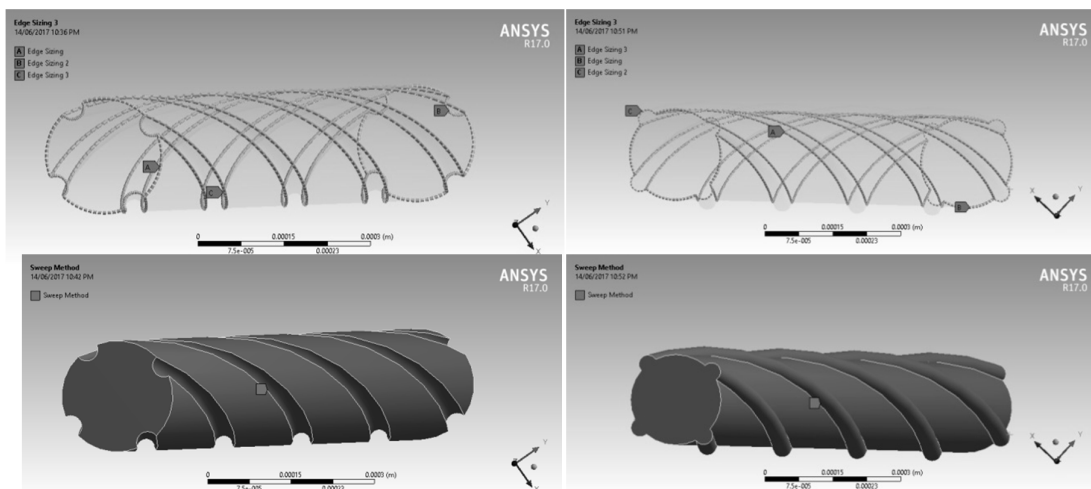


Fig. 2. Mesh Sizing and Method of the Geometries

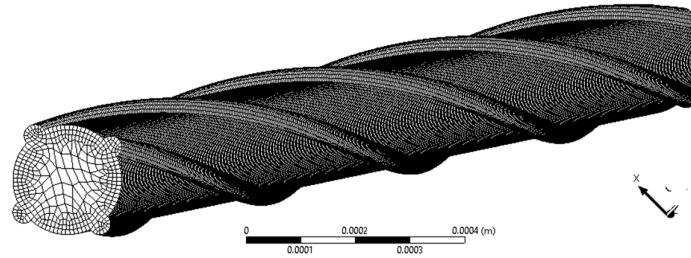


Fig. 3. Mesh of Grooved Pipe Fluid Geometry

The sizing method adopted in this study is using sweep method which is proven to be accurate for cylindrical type of geometries. It will then sweep the initially defined face mesh with edge sizing represented by the cross-section of the helically ribbed and grooved pipe through the body, spacing it by an incremental dimension through the defined number of divisions along the body of the geometry as shown in Fig. 3.

2.3 Mathematical modelling

In this study, the fluid used is 0%, 1%, 2% and 3% concentrations of Al_2O_3 /water nanofluid. The inlet and outlet condition used in the calculations are velocity-inlet and pressure-outlet. Inlet fluid temperature is assumed as $T_{\infty}=300.15$ K and constant heat flux of $q_{wall}=5000$ W/m².K is applied at the fluid surface. The solid pipe material is assumed to be aluminum with default thermophysical properties adopted from the software. The assumptions made are;(1) The fluid is incompressible and the fluid flow is in steady state; (2) The flow is laminar; (3) The radiation heat transfer is neglected; (4) The body force is neglected; (5) The electrostatic force is neglected (6) The thermal properties of solid and fluid are assumed to be constant. The governing equations in the Cartesian tensor form are[24] :

Continuity equation

$$\frac{\delta}{\delta x_i} (\rho_f u_i) = 0 \quad (1)$$

Momentum equation

$$\frac{\delta}{\delta x_i} (\rho_f u_i u_j) = -\frac{\delta \rho}{\delta x_j} + \frac{\delta}{\delta x_i} \left[\mu_f \left(\frac{\delta u_j}{\delta x_i} + \frac{\delta u_i}{\delta x_j} \right) \right] \quad (2)$$

Energy Equation

$$\frac{\delta}{\delta x_i} (\rho_f u_i c_{pf} T) = \frac{\delta}{\delta x_i} \left(k_i \frac{\delta T}{\delta x_i} \right) + \mu_f \left[2 \left(\frac{\delta u_i}{\delta x_i} \right)^2 + \left(\frac{\delta u_f}{\delta x_f} + \frac{\delta u_i}{\delta x_i} \right)^2 \right] \quad (3)$$

Reynolds number for the fluid geometry was set at 100, 300, 500, 800 and 1000 accordingly and the corresponding inlet velocity of the fluid is calculated according to its hydraulic diameter as shown in Table 3. The initial velocity of each different type of Reynolds number was calculated using equation (4).

$$U_{initial} = \frac{(Re \cdot \mu)}{(\rho_{fluid} \cdot D_h)} \quad (4)$$

$U_{initial}$ is defined as inlet velocity; Re is Reynold number, μ is viscosity, ρ is density, and D_h , is hydraulic diameter. In order to determine the cross-section of the helically grooved and ribbed microtube, the hydraulic diameter, D_h , was calculated by using equation (5),

$$D_h = \frac{4A}{P} \quad (5)$$

where A is the cross sectional area of the helically ribbed or grooved pipe and P is the wetted perimeter of the cross section. The pressure drop was calculated based on data at inlet and outlet by using equation (6)

$$\Delta P = P_{inlet} - P_{outlet} \quad (6)$$

The friction factor formula is given as (7)

$$f = \frac{2D_h \cdot \Delta P}{L \cdot \rho \cdot U^2} \quad (7)$$

where L is defined by the length of the pipe, ρ is the density of the fluid and U^2 is the product of initial velocity. The heat transfer coefficient is calculated using:

$$h = q_{in} / (T_s - T_f) \quad (8)$$

where is T_s surface temperature at the fluid while T_f is the bulk temperature of the fluid along the centerline of the geometry.

The Nusselt number in the present study were calculated as follow:

$$Nu = \frac{h \cdot D_h}{k} \quad (9)$$

where h is heat transfer coefficient, D_h is the hydraulic diameter and k is the thermal conductivity of the fluid.

2.3.1 Thermal properties of nanofluid

The thermophysical properties of nanofluids listed in this study are calculated using the following equations (10), (11), (12) and (13) which similarly reported by Azmi *et al.* [25]. The thermophysical properties of the nanofluid used in this study is shown in Table 2.

Density:

$$\rho_{nf} = \left(\frac{\phi}{100}\right) \rho_p + \left(1 - \frac{\phi}{100}\right) \rho_f \quad (10)$$

Specific Heat Capacity:

$$C_{nf} = \frac{\left(\frac{\phi}{100}\right)(\rho C)_p + \left(1 - \frac{\phi}{100}\right)(\rho C)_f}{\rho_{nf}} \quad (11)$$

Thermal Conductivity:

$$k_r = \frac{k_{nf}}{k_f} = 0.8938 \left(1 + \frac{\phi}{100}\right)^{1.37} \left(1 + \frac{T_{nf}}{70}\right)^{0.2777} \left(1 + \frac{d_p}{150}\right)^{-0.0336} \left(\frac{\alpha_p}{\alpha_f}\right)^{0.01737} \quad (12)$$

Viscosity:

$$\mu_r = \frac{\mu_{nf}}{\mu_f} = \left(1 + \frac{\phi}{100}\right)^{11.3} \left(1 + \frac{T_{nf}}{70}\right)^{-0.038} \left(1 + \frac{d_p}{170}\right)^{-0.061} \quad (13)$$

Table 2:

Properties of Al₂O₃/water nanofluid

ϕ	$\rho_{nf}(\text{kg/m}^3)$	$\mu_{nf}(\text{Mpa. s})$	$C_{nf}(\text{J/kg. K})$	$k_{nf}(\text{W/m. K})$
0%	997.7	0.949	4178.90	0.600
1%	1027.4	1.020	4046.96	0.617
2%	1057.2	1.130	3922.46	0.635
3%	1086.9	1.260	3804.78	0.653

Table 3:

Inlet velocity of Different Properties with Geometries

Reynolds No.	Initial Velocity(m/s)							
	Helically Ribbed Pipe				Helically Grooved Pipe			
	0%	1%	2%	3%	0%	1%	2%	3%
100	0.514	0.537	0.578	0.627	0.514	0.537	0.578	0.627
300	1.542	1.610	1.733	1.880	1.542	1.610	1.733	1.880
500	2.571	2.683	2.889	3.133	2.571	2.683	2.889	3.133
800	4.113	4.293	4.622	5.013	4.113	4.293	4.622	5.013
1000	5.142	5.366	5.778	6.266	5.142	5.366	5.778	6.266

2.3.2 Numerical Model

The computational fluid dynamics code Fluent (Ansys 17.0) was used to solve this problem. The system of governing Equations (10)-(13) was solved by the control-volume approach. A second order upwind scheme was employed to discretize the convection terms, diffusion terms and other quantities resulting from the governing equations. Pressure and velocity were coupled using the Semi Implicit Method for Pressure Linked Equations (SIMPLE). During the iterative process, the residuals were carefully monitored. For all simulations performed in the present study, solutions were considered to have converged when the residuals resulting from the iterative process for all governing Equations (10)– (13) were lower than 10^{-7} [1].

2.4 Grid Independence Test

A careful checking for the grid independency was conducted among the two different geometries to ensure the validity and exactness of the numerical results. The mesh for each cycle is controlled by the number of divisions on the face of the geometry under sweeping method. Fig. 4(a) and 4(b) illustrates the computed pressure drop versus grid density for the ribbed and grooved microtube using default liquid water from the software at Re of 100. It is clarified that the refinement after a mesh with 400,000 elements does not effect on the values of the pressure drop for ribbed pipe and mesh with 200,000 elements for grooved pipe geometry.

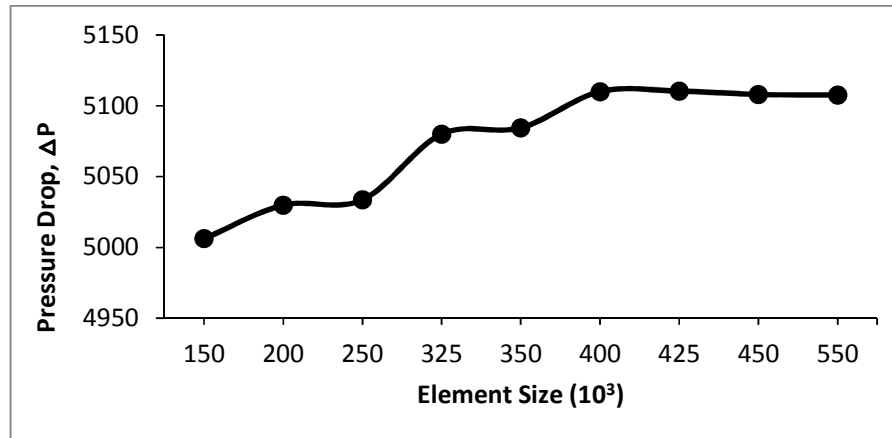


Fig. 4(a). Grid Independent Test for Ribbed Geometry

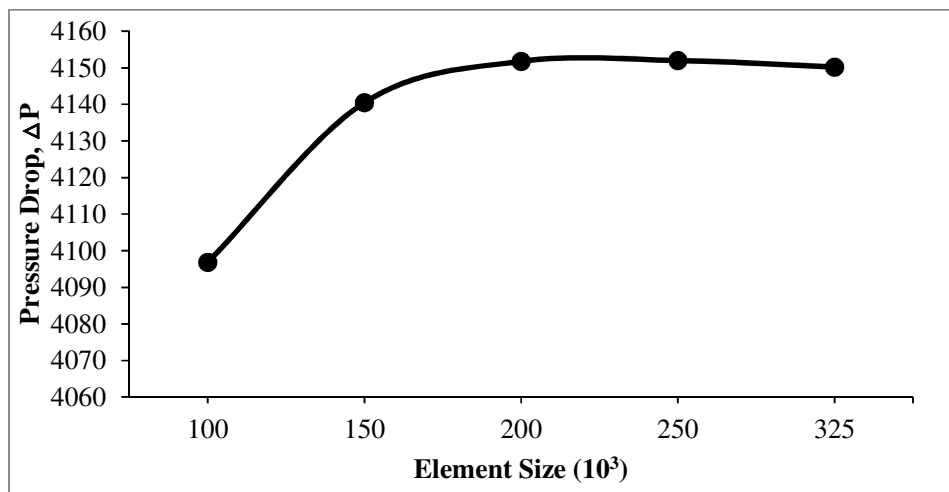


Fig. 4(b). Grid Independent Test for Grooved Geometry

3. Results and Discussion

In this study, heat transfer performance in helically ribbed and grooved microtube is analysed based on Nusselt number and comparison in pressure drop. Nusselt number is defined as dimensionless parameter that provides a comparison rate for how fast heat is transferred between materials where convection is taking place, as compared to basic heat transfer by conduction where

little internal movement of matter is occurring.

Piotr[1] in his studies have mentioned that taking hydraulic diameter for boundaries calculations will obtain a lower friction factor than a smooth pipe which is similar to this study. These results are not proper because in this case, both grooved and ribbed microtube would have lower pressure drop than on a smooth one. Many researchers (e.g. Brognaux *et al.*[26]) observed this problem and Webb and Scott[27] formulated a concept of the equivalent diameter, i.e. the diameter, which would exist if all the micro-fins were melted down and the material came back to the tube wall. Assumption of a constant cross sectional area of the tube for Piotr research would not be correct because every tested tube had different area of heat transfer (related with dimensions of grooves) and each pipe would also have a different equivalent diameter. Therefore Piotr, for the studied micro-finned tubes, has calculated a diameter equal to that of a smooth pipe – with the same cross-sectional area. Thus, the hydraulic diameter for the considered cases was equivalent with the plain tube.

For the present study however, the hydraulic diameter has been used for all the calculations since the comparison is done for helically ribbed and grooved pipe. The hydraulic diameter for helically ribbed pipe is 185 μm and the hydraulic diameter of helically grooved pipe is 165 μm . Thus, these pipes are not compared with smooth pipe. However, equivalent diameter with smooth pipe with 200 μm diameter will results in higher value of heat transfer between these geometries but the study is kept for future work.

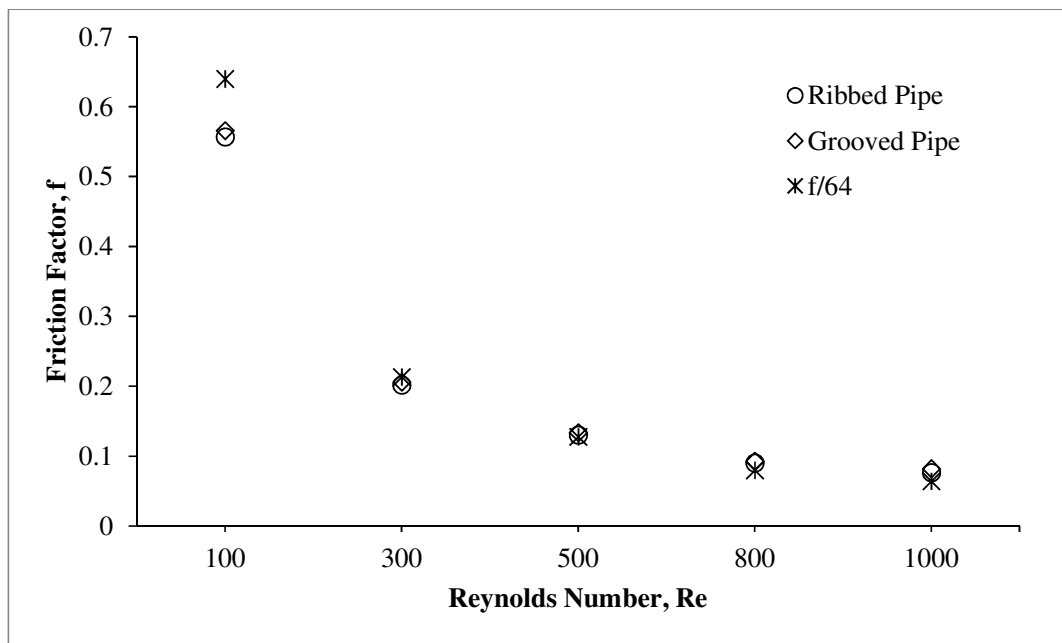


Fig. 5(a). Friction factor vs Reynolds number for both geometries

Fig. 5(a) shows the friction factor differences between both geometries using different Reynolds number with similar base fluid compared with theoretical laminar flow $f=64/Re$. At the lower Reynolds the theoretical value is higher than the roughened pipe value, however, when the Reynold number is higher, the grooved geometry shows slightly higher friction factor than ribbed geometry and theoretical value. Abubakar[28] found that as uniform inlet velocity is applied at the tube inlet, it takes an interval of time for the flow to be fully developed flow inside the microchannel the phenomena behind this is because of the developing boundary layer at the channel inlet. The grooved

pipe hydraulic diameter however is lower than the ribbed pipe hydraulic diameter thus observing higher friction factor. However, this method can be used to control the friction in microchannel.

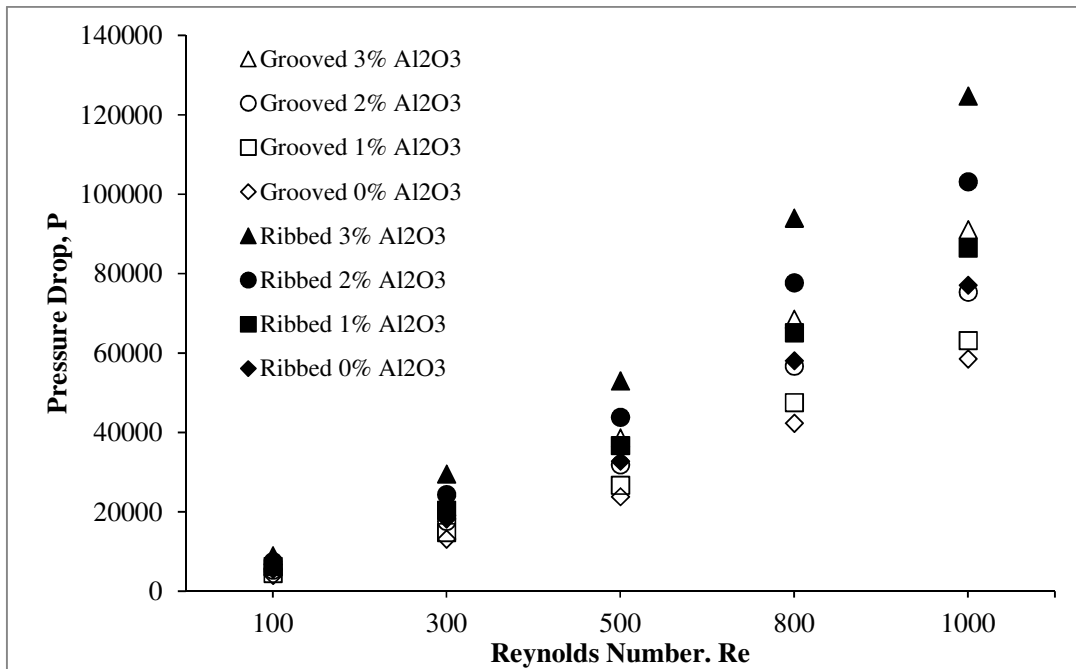


Fig. 5(b). Pressure Drop vs Reynolds number for both geometries

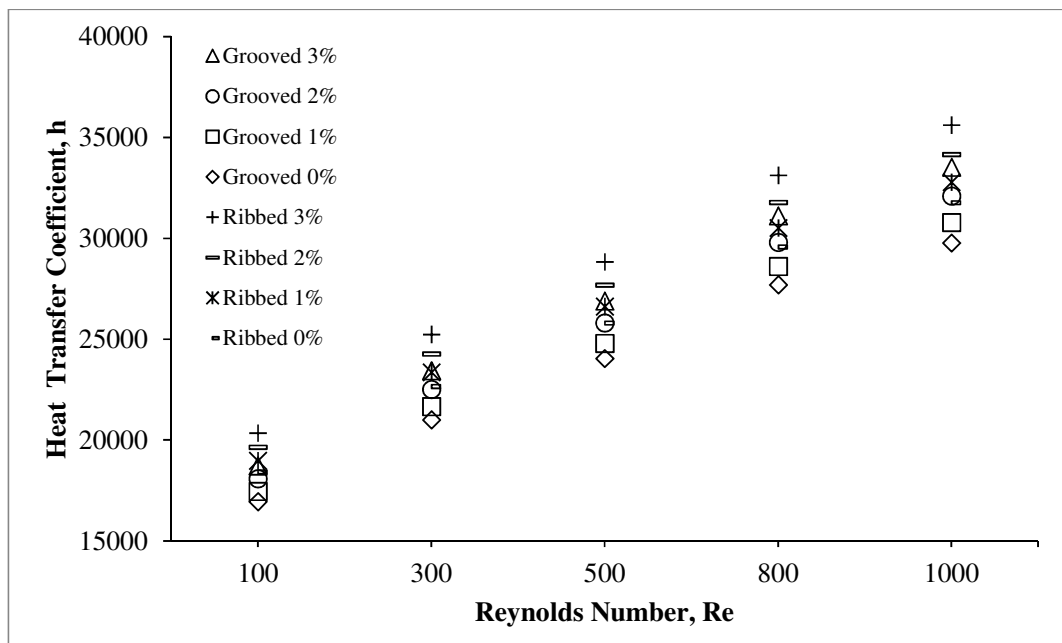


Fig. 5(c). Heat Transfer Coefficients vs Reynolds number for both geometries

However, Fig. 5(b) shows the increase in pressure drop values becomes more accentuated as the Reynolds number increases. This observation suggests that the use of nanofluid is a very effective method of increasing the pressure drop of the fluid since the changes in thermophysical properties

of different concentrations of nanofluid has been observed with increment in pressure drop[29]. Though at higher volume fractions increase in pressure drop is significant and it is important to find the optimum volume fraction for each application. Pressure drop at helically ribbed pipe observed higher than helically grooved pipe with maximum pressure drop is with 3% Al_2O_3 .

The heat transfer coefficients for the both geometries increase with the increment of the Reynolds number as shown in Fig. 5(c). Ribbed pipe exhibits higher heat transfer coefficients than grooved pipe. The effect of nanofluid however is seen where the maximum heat transfer coefficients is observed at Al_2O_3 3% nanofluid. This is due to the change in thermophysical properties of the nanofluid. Ding *et al.* [22] has found that migration of nanoparticles and the subsequent disturbance of the boundary layer were attributed to the enhancement in heat transfer rate. The presence of helical rib and grooves possibly promotes the dispersion and random movement of the particles, resulting in a better mixing of based fluid and nanoparticles near the tube wall.

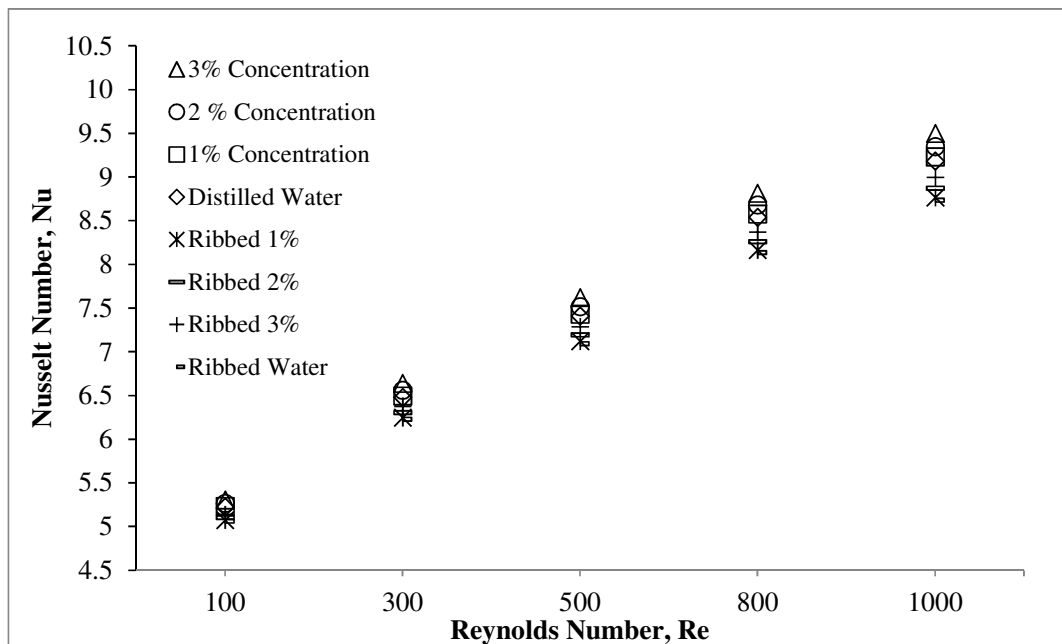


Fig. 5(d). Heat Transfer Coefficients vs Reynolds number for both geometries

Fig. 5(d) demonstrates the thermal performance of helically ribbed and grooved pipe represented by the Nusselt number. The figure clearly shows that grooved pipe has higher thermal efficiency than helically ribbed pipe. Even though, the heat transfer rate of ribbed pipe is found higher in figure 5(c), due to the differences of hydraulic diameter, grooved pipe emerges with higher Nusselt number. Bianco *et al.*[30] for the same type of flow and boundary condition, found single phase model to predict heat transfer coefficient within 11% difference. This is considered to be good result according to them as this will be useful to test new nanofluids.

4. Conclusion

Numerical simulation on laminar nanofluid flow inside helically ribbed and grooved microtube is presented in this paper. The effects of using Al_2O_3 /water nanofluids with different volume fractions on the heat transfer enhancement of both geometries are studied. Based on the presented results, the following conclusions can be drawn:

- I. As uniform inlet velocity is applied at the channel inlet, it takes an interval of time for the flow to be fully developed flow inside the microchannel. The phenomena behind this is because of the developing boundary layer at the channel inlet.
- II. Pressure drop for helically ribbed pipe is higher than helically grooved pipe.
- III. Al_2O_3 with volume fraction 3% provides the maximum temperature reduction of 0.4% compare to using pure water as working fluid.
- IV. The simulated results showed that the heat transfer performance of Al_2O_3 with 3% was better than that of Al_2O_3 with 1%, of Al_2O_3 with 2%, and distilled water. Increasing the thermal conductivity of working fluid enhanced the heat transfer performance of microchannel heat sink. Al_2O_3 is recommended to achieve overall heat transfer enhancement.

References

- [1] P. Jasiński, "Numerical study of friction factor and heat transfer characteristics for single-phase turbulent flow in tubes with helical micro-fins," *Archive of Mechanical Engineering*, vol. 59, no. 4, pp. 469-485, 2012.
- [2] S. Pal and S. K. Saha, "Laminar fluid flow and heat transfer through a circular tube having spiral ribs and twisted tapes," *Experimental Thermal and Fluid Science*, vol. 60, pp. 173-181, 2015.
- [3] Y. Wang, B. Zhou, Z. Liu, Z. Tu, and W. Liu, "Numerical study and performance analyses of the mini-channel with discrete double-inclined ribs," *International Journal of Heat and Mass Transfer*, vol. 78, pp. 498-505, 2014.
- [4] S. K. Saha, "Thermal and friction characteristics of laminar flow through rectangular and square ducts with transverse ribs and wire coil inserts," *Experimental Thermal and Fluid Science*, vol. 34, no. 1, pp. 63-72, 2010.
- [5] W. Peng, P.-X. Jiang, Y.-P. Wang, and B.-Y. Wei, "Experimental and numerical investigation of convection heat transfer in channels with different types of ribs," *Applied Thermal Engineering*, vol. 31, no. 14, pp. 2702-2708, 2011.
- [6] T.-M. Jeng, S.-C. Tzeng, and C.-H. Lin, "Heat transfer enhancement of Taylor–Couette–Poiseuille flow in an annulus by mounting longitudinal ribs on the rotating inner cylinder," *International Journal of Heat and Mass Transfer*, vol. 50, no. 1, pp. 381-390, 2007.
- [7] T. Ravigururajan and A. Bergles, "Development and verification of general correlations for pressure drop and heat transfer in single-phase turbulent flow in enhanced tubes," *Experimental Thermal and Fluid Science*, vol. 13, no. 1, pp. 55-70, 1996.
- [8] M. Siddique and M. Alhazmy, "Experimental study of turbulent single-phase flow and heat transfer inside a micro-finned tube," *International Journal of refrigeration*, vol. 31, no. 2, pp. 234-241, 2008.
- [9] D. H. Han and K.-J. Lee, "Single-phase heat transfer and flow characteristics of micro-fin tubes," *Applied Thermal Engineering*, vol. 25, no. 11, pp. 1657-1669, 2005.
- [10] H. Li, K. Ye, Y. Tan, and S. Deng, "Investigation on tube-side flow visualization, friction factors and heat transfer characteristics of helical-ridging tubes," *Heat Transfer*, vol. 3, pp. 75-80, 1982.
- [11] S. Al-Fahed, L. Chamra, and W. Chakroun, "Pressure drop and heat transfer comparison for both microfin tube and twisted-tape inserts in laminar flow," *Experimental Thermal and Fluid Science*, vol. 18, no. 4, pp. 323-333, 1998.
- [12] A. M. Hussein, K. Sharma, R. Bakar, and K. Kadirgama, "A review of forced convection heat transfer enhancement and hydrodynamic characteristics of a nanofluid," *Renewable and Sustainable Energy Reviews*, vol. 29, pp. 734-743, 2014.
- [13] A. M. Hussein, K. V. Sharma, R. Bakar, and K. Kadirgama, "The effect of cross sectional area of tube on friction factor and heat transfer nanofluid turbulent flow," *International Communications in Heat and Mass Transfer*, vol. 47, pp. 49-55, 2013.
- [14] M. E. Meibodi, M. Vafaie-Sefti, A. M. Rashidi, A. Amrollahi, M. Tabasi, and H. S. Kalal, "An estimation for velocity and temperature profiles of nanofluids in fully developed turbulent flow conditions," *International Communications in Heat and Mass Transfer*, vol. 37, no. 7, pp. 895-900, 2010.
- [15] A. M. Hussein, R. Bakar, and K. Kadirgama, "Study of forced convection nanofluid heat transfer in the automotive cooling system," *Case Studies in Thermal Engineering*, vol. 2, pp. 50-61, 2014.
- [16] A. M. Hussein, K. Sharma, R. Bakar, and K. Kadirgama, "The effect of nanofluid volume concentration on heat transfer and friction factor inside a horizontal tube," *Journal of Nanomaterials*, vol. 2013, p. 1, 2013.
- [17] T. Maré, S. Halefadi, S. Van Vaerenbergh, and P. Estellé, "Unexpected sharp peak in thermal conductivity of carbon nanotubes water-based nanofluids," *International communications in heat and mass transfer*, vol. 66, pp. 80-83, 2015.

- [18] Y.-T. Yang, H.-W. Tang, B.-Y. Zeng, and C.-H. Wu, "Numerical simulation and optimization of turbulent nanofluids in a three-dimensional rectangular rib-grooved channel," *International Communications in Heat and Mass Transfer*, vol. 66, pp. 71-79, 2015.
- [19] C. Y. Tso, S. C. Fu, and C. Y. Chao, "A semi-analytical model for the thermal conductivity of nanofluids and determination of the nanolayer thickness," *International Journal of Heat and Mass Transfer*, vol. 70, pp. 202-214, 2014.
- [20] G. Bourantas and V. C. Loukopoulos, "Modeling the natural convective flow of micropolar nanofluids," *International Journal of Heat and Mass Transfer*, vol. 68, pp. 35-41, 2014.
- [21] S. Murshed, K. Leong, and C. Yang, "Enhanced thermal conductivity of TiO₂—water based nanofluids," *International Journal of thermal sciences*, vol. 44, no. 4, pp. 367-373, 2005.
- [22] D. Wen and Y. Ding, "Experimental investigation into convective heat transfer of nanofluids at the entrance region under laminar flow conditions," *International journal of heat and mass transfer*, vol. 47, no. 24, pp. 5181-5188, 2004.
- [23] S. Z. Heris, S. G. Etemad, and M. N. Esfahany, "Experimental investigation of oxide nanofluids laminar flow convective heat transfer," *International Communications in Heat and Mass Transfer*, vol. 33, no. 4, pp. 529-535, 2006.
- [24] L. Chai, G. D. Xia, and H. S. Wang, "Numerical study of laminar flow and heat transfer in microchannel heat sink with offset ribs on sidewalls," *Applied Thermal Engineering*, vol. 92, pp. 32-41, 2016.
- [25] W. Azmi, K. Sharma, P. Sarma, R. Mamat, S. Anuar, and V. D. Rao, "Experimental determination of turbulent forced convection heat transfer and friction factor with SiO₂ nanofluid," *Experimental Thermal and Fluid Science*, vol. 51, pp. 103-111, 2013.
- [26] L. J. Brognaux, R. L. Webb, L. M. Chamra, and B. Y. Chung, "Single-phase heat transfer in micro-fin tubes," *International Journal of Heat and Mass Transfer*, vol. 40, no. 18, pp. 4345-4357, 1997.
- [27] R. Webb and M. Scott, "A parametric analysis of the performance of internally finned tubes for heat exchanger application," *ASME J. Heat Transfer*, vol. 102, pp. 38-43, 1980.
- [28] S. Abubakar and N. C. Sidik, "Numerical prediction of laminar nanofluid flow in rectangular microchannel heat sink," *J. Adv. Res. Fluid Mech. Therm. Sci.*, vol. 7, no. 1, pp. 29-38, 2015.
- [29] S. Li and J. Eastman, "Measuring thermal conductivity of fluids containing oxide nanoparticles," *J. Heat Transf.*, vol. 121, no. 2, pp. 280-289, 1999.
- [30] V. Bianco, F. Chiacchio, O. Manca, and S. Nardini, "Numerical investigation of nanofluids forced convection in circular tubes," *Applied Thermal Engineering*, vol. 29, no. 17, pp. 3632-3642, 2009.